Gold helix photonic metamaterials: A numerical parameter study

Justyna K. Gansel[1], Martin Wegener[1,2], Sven Burger[3], and Stefan Linden[1,2]

[1]*Institut für Angewandte Physik and DFG-Center for Functional Nanostructures (CFN), Karlsruhe Institute of Technology (KIT), D-76128 Karlsruhe, Germany*

[2]*Institut für Nanotechnologie,Karlsruhe Institute of Technology (KIT), Hermann-von-Helmholtz-Platz 1, D-76344 Eggenstein-Leopoldshafen, Germany*

[3]*Zuse Institute Berlin, Takustrasse 7, D-14195 Berlin, Germany and DFG Forschungszentrum Matheon, Strasse des 17. Juni 136, D-10623 Berlin, Germany*

**Justyna.Gansel@physik.uni-karlsruhe.de*

Abstract: We have recently shown that metamaterials composed of three-dimensional gold helices periodically arranged on a square lattice can be used as compact "thin-film" circular polarizers with one octave bandwidth. The physics of the motif of these artificial crystals is closely related to that of microwave sub-wavelength helical antennas in end-fire geometry. Here, we systematically study the dependence of the metamaterial's chiral optical properties on helix pitch, helix radius, two-dimensional lattice constant, wire radius, number of helix pitches, and angle of incidence. Our numerical calculations show that the optical properties are governed by resonances of the individual helices, yet modified by interaction effects. Furthermore, our study shows possibilities and limitations regarding performance optimization.

OCIS codes: (160.1585) Materials: Chiral media; (160.3918) Materials: Metamaterials; (260.5430) Physical optics: Polarization.

References and links

1. E. Hecht, *Optics* (Addison-Wesley, San Francisco, 2002, 4th edition).
2. K. F. Lindman, "Über eine durch ein isotropes System von spiralförmigen Resonatoren erzeugte Rotationspolarisation der elektromagnetischen Wellen," Ann. Phys. **368**(23), 621–644 (1920).
3. J. K. Gansel, M. Thiel, M. S. Rill, M. Decker, K. Bade, V. Saile, G. von Freymann, S. Linden, and M. Wegener, "Gold helix photonic metamaterial as broadband circular polarizer," Science **325**(5947), 1513–1515 (2009).
4. P. A. Belov, C. R. Simovski, and S. A. Tretyakov, "Example of bianisotropic electromagnetic crystals: the spiral medium," Phys. Rev. E Stat. Nonlin. Soft Matter Phys. **67**(5), 056622 (2003).
5. M. G. Silveirinha, "Design of linear-to-circular polarization transformers made of long densely packed metallic helices," IEEE Trans. Antenn. Propag. **56**(2), 390–401 (2008).
6. R. Abdeddaïm, G. Guida, A. Priou, B. Gallas, and J. Rivory, "Negative permittivity and permeability of gold square nanospirals," Appl. Phys. Lett. **94**(8), 081907 (2009).
7. Z.-Y. Zhang, and Y.-P. Zhao, "Optical properties of helical and multiring Ag nanostructures: The effect of pitch height," J. Appl. Phys. **104**(1), 013517 (2008).
8. J. D. Kraus, and R. J. Marhefka, *Antennas: For All Applications* (McGraw-Hill, New York, 2003, 3rd edition).
9. H.-S. Kitzerow, and C. Bahr, eds., *Chirality in Liquid Crystals* (Springer, Heidelberg, 2001, 1st edition).
10. M. Thiel, G. von Freymann, and M. Wegener, "Layer-by-layer three-dimensional chiral photonic crystals," Opt. Lett. **32**(17), 2547–2549 (2007).
11. M. Thiel, M. Decker, M. Deubel, M. Wegener, S. Linden, and G. von Freymann, "Polarization stop bands in chiral polymeric three-dimensional photonic crystals," Adv. Mater. **19**(2), 207–210 (2007).
12. www.cst.com/Content/Products/MWS/Overview.aspx
13. www.lumerical.com
14. www.jcmwave.com
15. I. V. Lindell, A. H. Sihvola, S. A. Tretyakov, and A. J. Viitanen, *Electromagnetic Waves in Chiral and Bi-Isotropic Media* (Artech House, Boston, 1994).
16. D. H. Kwon, D. H. Werner, A. V. Kildishev, and V. M. Shalaev, "Material parameter retrieval procedure for general bi-isotropic metamaterials and its application to optical chiral negative-index metamaterial design," Opt. Express **16**(16), 11822–11829 (2008).

#119965 - $15.00 USD Received 13 Nov 2009; revised 22 Dec 2009; accepted 28 Dec 2009; published 7 Jan 2010

1. Introduction

In some optics textbooks [1], fictitious materials composed of metal helices are considered as a paradigm for explaining on a classical footing optical activity arising from structural chirality. In 1920, Karl Lindman realized and characterized such metal helix structures at microwave frequencies [2]. Recently, artificial uniaxial materials composed of three-dimensional gold helices arranged on a square lattice ("metamaterials") have become experimental reality [3] at infrared wavelengths. The structure is illustrated in Fig. 1. For propagation of light along the helix axis, such structures offer giant circular dichroism. In particular, they can act as compact "thin-film" (two sub-wavelength helix pitches) circular polarizers – with spectral bandwidths exceeding one octave. Thus, these structures can be viewed as the circular analogues of the well-known wire-grid broadband linear polarizers that have found widespread commercial use, e.g., in Fourier transform spectrometers.

Previous theoretical work on helix-based metamaterials [4–6] and on individual silver helices with nanometer dimensions [7] has pointed out a variety of interesting aspects, however, it has not addressed optimizing the structure with respect to the above application. In this letter, we present a systematic numerical study on the dependence on all relevant structure parameters. Our study further clarifies the nature of the underlying optical resonances and shows possibilities and limitations regarding structure optimization.

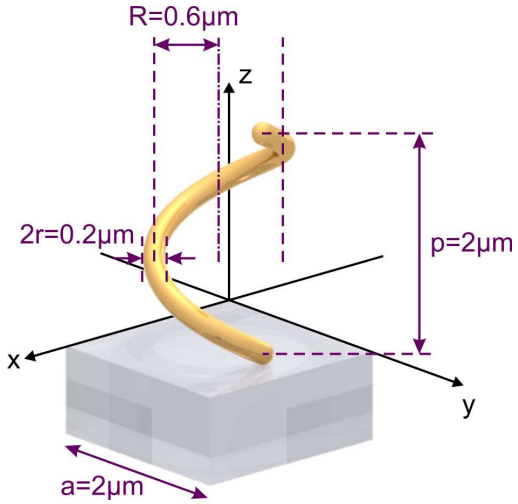

Fig. 1. Scheme of one lateral unit cell of a chiral metamaterial composed of left-handed gold helices arranged in a square lattice on a glass substrate. The relevant structure parameters are illustrated. We consider propagation of light along the helix axis. $N = 1$ helix pitch is shown.

The motif of our metamaterial structure is related to helical antennas in the so-called end-fire geometry [8]. Such helical antennas are, e.g., widely used in microwave wireless local-area network (WLAN) applications. Figure 1 illustrates the underlying metal helix with radius R, wire radius r, pitch (or axial period) p, and number of pitches N. Antenna theory predicts that a circularly polarized wave is emitted along the helix axis. Optimum performance requires that the pitch angle [8] φ given by $\tan(\varphi) = p/(2\pi R)$ is around φ = 12-14 degrees. This is equivalent to a pitch of about $p \approx 0.73 \times 2R$. Furthermore, provided that the wire is thin ($r << R$) and that at least $N = 3$ helix pitches are used, antenna theory states that the free-space operation wavelength λ is in the interval

$$\lambda \in 2\pi R \times \left[\frac{3}{4}, \frac{4}{3}\right]. \qquad (1)$$

#119965 - $15.00 USD Received 13 Nov 2009; revised 22 Dec 2009; accepted 28 Dec 2009; published 7 Jan 2010

According to (1), this leads to a ratio of maximum to minimum wavelength of 16/9, which is close to one octave – a fairly broad bandwidth for an antenna. Obviously, the helical antenna is a sub-wavelength antenna as the free-space operation wavelength is between 4.7 and 8.4 times larger than the helix radius R. Notably, under the above conditions, the helical antenna operation wavelength neither depends on the length of the antenna (i.e., on the number of helix pitches) nor on the helix pitch p alone. For infinitely many helix turns N, one obtains perfectly circularly polarized emission. In the language of antenna theory, the on-axis "axis ratio" AR (which is given by the ratio of the major and minor radius of the polarization ellipse) [8] becomes unity. For finite values of N, the axis ratio scales according to $AR = (2N + 1)/(2N)$ [8].

If, for example, an electrical current in a left-handed helical "sender" antenna leads to emission of a left-handed circularly polarized electromagnetic wave propagating along the helix axis, an incident wave with the same handedness propagating along the helix axis is expected to induce an electrical current in an identical "receiver" antenna, i.e., it will interact with the antenna. In contrast, the other handedness of light is not expected to interact with the antenna. Thus, a two-dimensional square array of helical antennas with a certain lattice constant, a, will lead to reflection and/or absorption of light incident onto the array if the handedness of the light is identical to that of the helices. If metal losses are negligible, absorption does not occur and all light that is not transmitted will be reflected. In contrast, light with the opposite circular handedness will be transmitted. In this reasoning, we have tacitly assumed that the lateral interaction among the different metal helices in the two-dimensional array is negligible. Indeed, on page 225 of [8], the inventor of the helical antenna, John Kraus, states in boldface: "… Not only does the helix have a nearly uniform resistive input over a wide bandwidth but it also operates as a 'supergain' end-fire array over the same bandwidth! Furthermore, it is noncritical with respect to conductor size and turn spacing. It is also easy to use in arrays because of almost negligible mutual impedance …". We will see below that the latter assumption is not quite correct under our conditions. Nevertheless, the qualitative behavior does remain for arrays of helices.

In the language of solid-state physics, this unusual broadband operation originates from the interaction between the different helix pitches [3] within one helix. It has been shown [3] that a single pitch of a metal helix exhibits several pronounced and sharp resonances. Two of these resonances are within the effective-medium limit in the sense that no diffraction occurs for incident light propagation along the helix axis. For two and more helix pitches, these two resonances evolve into a broad band [3], the minimum and maximum frequencies of which roughly correspond to the positions of the two sharp resonances. This behavior is analogous to that of discrete atomic levels evolving into broad electronic bands in a crystalline solid. The width of the band is determined by the interaction among the atoms. In analogy, the width of the band for our metamaterial structure is determined by the interaction among the different helix pitches within one helix. In other words: Bragg reflection/resonance influences the behavior. However, the behavior is still quite different from that of cholesteric liquid crystals [9], which can essentially be viewed as a layered twisted *dielectric* structure [10]. The behavior is also different from helical dielectric structures [11]. There [9–11], the operation wavelength is directly proportional to the period along the propagation direction – in sharp contrast to what we will see below for the case of metal helices.

2. Numerical calculations

For the numerical calculations in this Letter, to check for consistency, we have intentionally used three different software packages: CST MICROWAVE STUDIO [12], based on a finite-integration technique (FIT), LUMERICAL [13], based on a finite-difference time-domain approach (FDTD), and JCMsuite [14], based on a frequency-domain finite-element method (FEM). All three packages have delivered consistent results. In all three cases, we employ periodic boundary conditions for the two-dimensional array. Precisely, in the FIT (FDTD)

#119965 - $15.00 USD Received 13 Nov 2009; revised 22 Dec 2009; accepted 28 Dec 2009; published 7 Jan 2010

calculations, we have used a mesh size ranging between 200 nm and 10 nm (between 50 nm and 4 nm) and a time step of 0.03 fs (0.0077 fs). For the FEM calculations, we have used second-order finite elements on unstructured tetrahedral grids with about 25000 elements. Element volumes range between about $(30\ \text{nm})^3$ and $(400\ \text{nm})^3$.

The results depicted in Figs. 2,3,5,6, and 8 are actually obtained by CST MICROWAVE STUDIO, those in Fig. 4 by LUMERICAL, and those in Fig. 7 by JCMsuite. Comparison of the black curves in these figures shows that the three software packages have delivered consistent results. We use realistic parameters [3] for the free-electron Drude model describing the gold optical properties: the plasma frequency is $\omega_{\text{pl}} = 1.37 \times 10^{16}$ rad/s and the collision frequency is $\omega_{\text{col}} = 1.2 \times 10^{14}$ rad/s. All calculations in this work with the notable exception of Fig. 7 assume propagation of light along the helix axis (see Fig. 1). To avoid artificial sharp edges, the ends of the gold wire are terminated by gold half spheres with radius r. All simulated metamaterial structures are located on a glass substrate (half-space geometry) with real refractive index $n = 1.5$. Light impinges from the air side. We show left- and right-handed circular polarization of the incident light and analyze the emerging polarization in terms of left- and right-handed circular polarization. We explicitly show results for left-handed gold helices. By symmetry, for right-handed helices, for all handedness of the incident and transmitted light, strictly identical results are obtained if "left" and "right" are consistently interchanged.

2.1 Varying the number of pitches N

Figure 2 shows the intensity transmittance and intensity conversion spectra versus the number of helix pitches N. The incident light has left-handed circular polarization (LCP) or right-handed circular polarization (RCP). Precisely, "transmittance" refers to the ratio of LCP (RCP) transmitted light intensity and LCP (RCP) incident light intensity. Similarly, "conversion" refers to the ratio of LCP (RCP) transmitted light intensity and RCP (LCP) incident light intensity. In Fig. 2, the parameters $R = 0.6$ µm, $r = 0.1$ µm, $a = 2$ µm, and $p = 2$ µm (compare Fig. 1) are fixed and intentionally identical to those in Fig. 1 of our previous work [3]. For yet longer wavelengths than the ones explicitly depicted in Fig. 2, no further resonances occur for axial propagation. For yet shorter wavelengths, diffraction of light into the substrate can occur, i.e., Wood anomalies are expected. This leads to a minimum wavelength given by the product of the substrate refractive index $n = 1.5$ times the lattice constant $a = 2$ µm, i.e., to 3 µm wavelength. Hence, for wavelengths shorter than this critical value, the structures can certainly no longer be viewed as an effective material and, furthermore, they can no longer be really used as a circular polarizer. Thus, throughout this article, we restrict ourselves to the spectral window of Fig. 2 (3 µm to 12 µm wavelength, equivalent to two octaves). For $N = 1$, two distinct and sharp resonances are found [3] for incident light with the same handedness as the helix. The other handedness is transmitted. For the long-wavelength resonance, the electrical current has nodes only at the ends of the metal wire; the short-wavelength resonance has one additional node in the middle of the wire. Starting from these resonances for $N = 1$, a broad and more or less unstructured transmittance minimum evolves with increasing N. This aspect, which has been discussed qualitatively above, connects to our previous work [3]. Here, we merely show more values of N than in [3]. Notably, the minimum and maximum wavelengths do not shift much with increasing N. This means that none of the resonances shifts proportional to the total length of the metal wire or proportional to the height of the structure, i.e., proportional to $N \times p$.

#119965 - $15.00 USD Received 13 Nov 2009; revised 22 Dec 2009; accepted 28 Dec 2009; published 7 Jan 2010

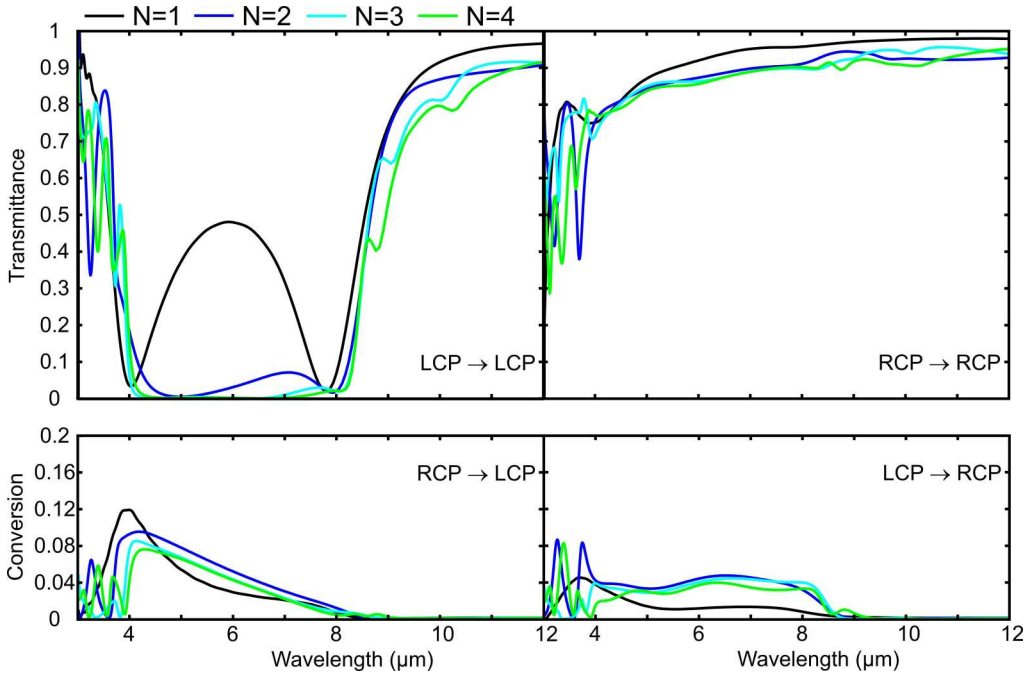

Fig. 2. Intensity transmittance and intensity conversion spectra (note the different vertical scales) for circularly polarized incident light propagating along the helix axis (compare Fig. 1). Results for left-handed circular polarization (LCP) and right-handed circular polarization (RCP) of light are shown. The metal helices are left-handed. Parameters are $R = 0.6$ μm, $r = 0.1$ μm, $a = 2$ μm, and $p = 2$ μm. The gold is described by the free-electron Drude model. The number of helix pitches, N, is varied as indicated.

Clearly, it is not helpful to start our further systematic parameter variations from this featureless broad band. Trends can rather be revealed when starting from the two pronounced resonances found for $N = 1$.

2.2 Varying the pitch height p

Figure 3 illustrates the dependence on helix pitch p for $N = 1$. The other parameters are fixed to their respective values in Fig. 2. It becomes obvious that the resonance positions do shift to some extent. However, while the pitch p varies by more than a factor of three, the resonance positions merely shift by some tens of percent. We can conclude that the physics of metal helices is quite distinct from that of dielectric helices with closely similar geometry [11] (see discussion above). For the dielectric helices in [11], the vacuum wavelength corresponding to the Bragg resonance has simply been proportional to the pitch height p. This means that the response of dielectric helices is dominated by the Bragg resonance, whereas that of the metal helices is determined by the interplay of pronounced internal resonances and their mutual coupling [3].

2.3 Varying the lattice constant a

The effect of the lateral interaction of the individual helices is investigated in Fig. 4 for $N = 1$. Here, the square lattice constant, a, is varied. All other parameters are fixed to their respective values in Fig. 2. The long-wavelength resonance shifts towards shorter wavelengths with decreasing lattice constant a. For this resonance [3], the current in the helix wire is flowing in

#119965 - $15.00 USD Received 13 Nov 2009; revised 22 Dec 2009; accepted 28 Dec 2009; published 7 Jan 2010

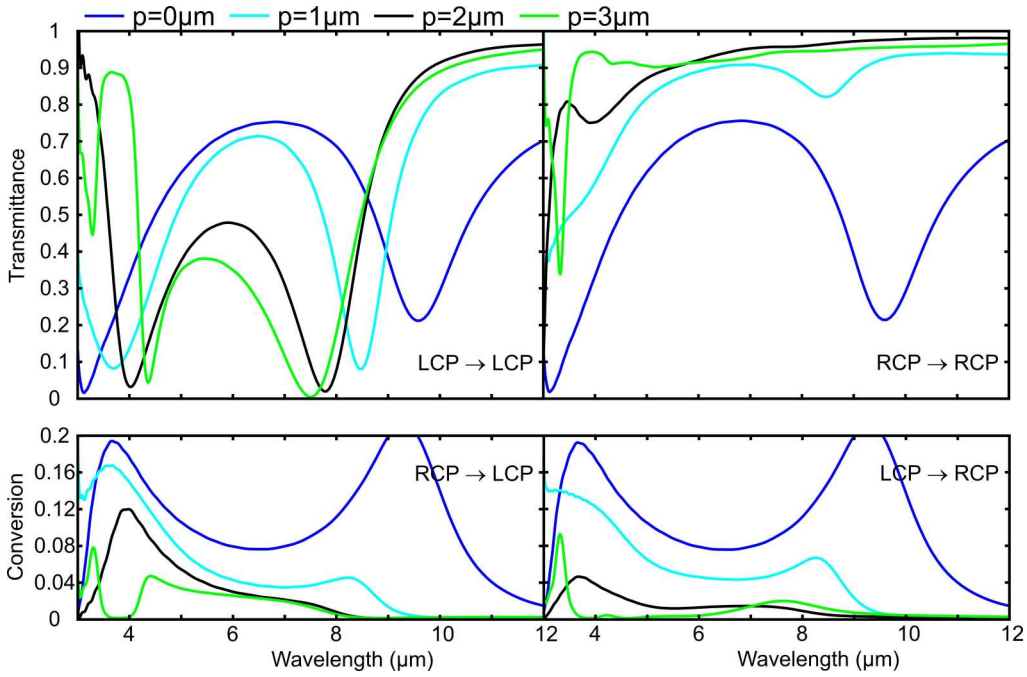

Fig. 3. As Fig. 2, $N = 1$, but the helix pitch, p, is varied as indicated. $p = 0$ μm corresponds to a planar, hence non-chiral, split-ring resonator with 100 nm gap width.

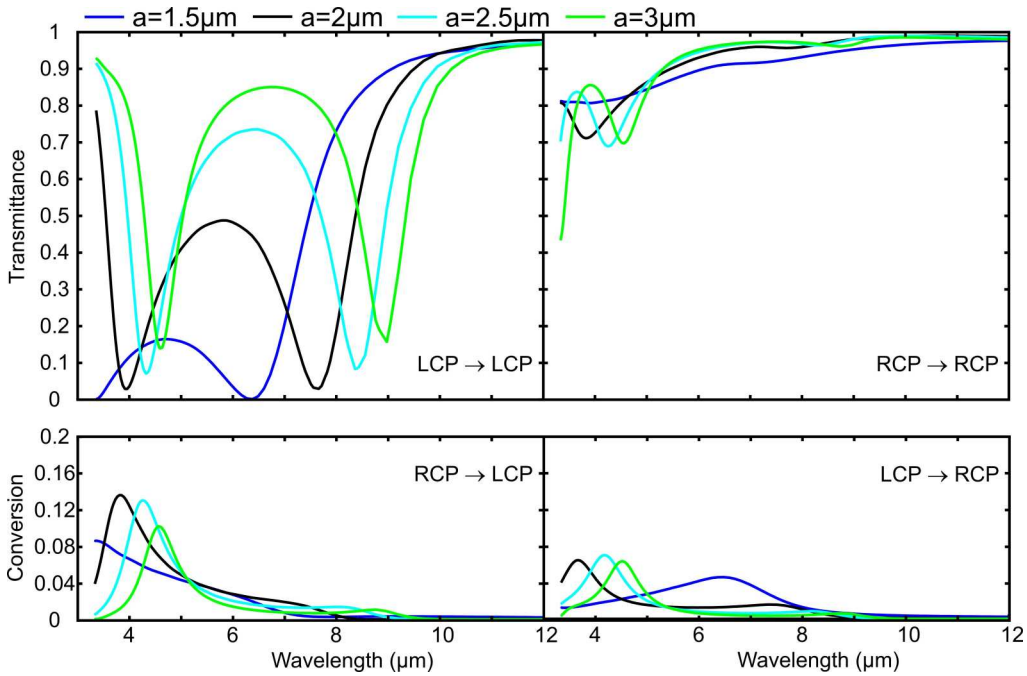

Fig. 4. As Fig. 2, $N = 1$, but the square lattice constant, a, is varied as indicated.

one direction at any point within an optical cycle. Thus, a snapshot of the magnetic field of this mode is similar to that of a permanent magnet. For two adjacent parallel oriented permanent magnets side by side, the energy increases with decreasing spacing as the two north (south) poles come closer and closer. This analogy qualitatively explains our numerical

#119965 - $15.00 USD Received 13 Nov 2009; revised 22 Dec 2009; accepted 28 Dec 2009; published 7 Jan 2010

findings. The shorter-wavelength mode with one additional current node [3] shifts in the same direction but neither by the same wavelength nor frequency difference as the long-wavelength resonance. For the shorter-wavelength resonance, the two parts of one helix have anti-parallel magnetic dipole moments but interact with their neighbors in the same qualitative (but not quantitative) fashion as described above. Furthermore, the depth of both resonances decreases when increasing the lattice constant. This aspect is simply due to the fact that the number of dipoles per area or per volume decreases. However, the overall qualitative behavior stays close to that of end-fire helical antennas described in the introduction. Optimum circular polarizer operation is expected for dense packing of the helices, i.e., for a being only slightly larger than the helix diameter $2R$. Nevertheless, a direct mechanical/electrical contact of adjacent metal helices should be avoided as this is expected to lead to very large deviations. For direct contact, the picture of separated antennas is definitely no longer applicable.

2.4 Varying the helix radius R

Following antenna theory, the strongest dependence of the resonance positions is expected when varying the helix radius R. Figure 5 investigates this aspect. Indeed, we find that the resonance wavelengths shift more or less proportional to R. Even the absolute positions of the resonance wavelengths roughly coincide with the prediction of antenna theory outlined in the introduction. Clearly, decreasing R while keeping the lattice constant a fixed dilutes the array, leading to more shallow resonances (compare Fig. 4).

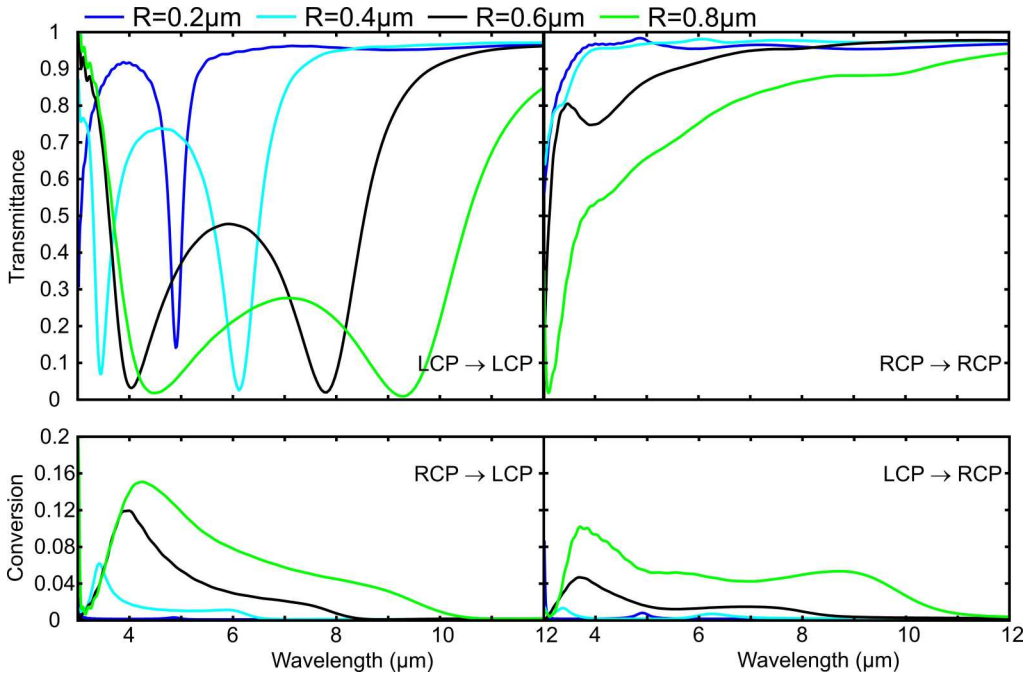

Fig. 5. As Fig. 2, $N = 1$, but the metal helix radius, R, is varied as indicated.

2.5 Varying the wire radius r

In Fig. 6, the radius of the metal wire, r, is varied. All other parameters are fixed to their respective values in Fig. 2. With increasing r, the resonances experience a slight shift towards shorter wavelengths. This trend can be understood by appreciating that the electrical current follows the shortest possible path, i.e., it mainly flows at the inner radius of the helix. Thus, increasing r effectively approximately reduces the helix radius R according to $R \rightarrow (R\text{-}r)$, the net effect of which corresponds to that shown in Fig. 5.

#119965 - $15.00 USD Received 13 Nov 2009; revised 22 Dec 2009; accepted 28 Dec 2009; published 7 Jan 2010

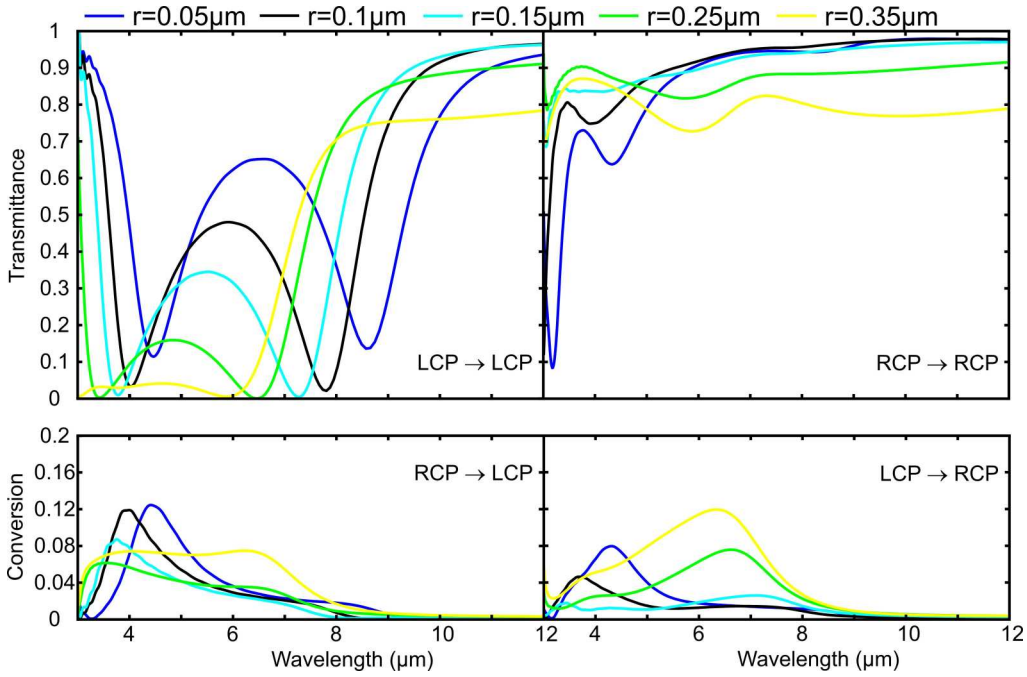

Fig. 6. As Fig. 2, $N = 1$, but the metal wire radius, r, is varied as indicated.

2.6 Dependence on angle of incidence α

The gold-helix metamaterial is designed for propagation of light along the helix axis. In any practical implementation, however, the incident light will have a certain angular spread. Figure 7 shows calculated transmittance spectra for angles of incidence with respect to the surface normal ranging from 0 to 40 degrees in steps of 10 degrees. Obviously, 10 degrees deviation from normal incidence does already significantly deteriorate the performance. This aspect needs to be considered in possible applications.

2.7 Conversion and reflectance

In discussing these trends, so far, we have focused on the resonance positions in the intensity transmittance spectra but we have completely neglected the behavior of the circular polarization intensity conversion that is also shown in Figs. 2-6. Recall that an ideal circular polarizer requires two aspects. (i) One incident circular polarization should be totally transmitted, whereas the other is completely blocked. (ii) The transmitted incident circular polarization should be maintained, i.e., polarization conversion should ideally be negligible if pure circularly polarized transmitted light is aimed at. In Figs. 2-6, depending on structure parameters, the circular intensity conversion can reach values as high as 17% (except for $p = 0$ μm in Fig. 3 which is not chiral, hence not relevant). For suitable parameter combinations, the intensity conversion stays below a few percent for the entire bandwidth of one octave.

Finally, we discuss the behavior of the intensity reflectance. While this aspect is not directly relevant for the applications we have in mind, the reflectance behavior is connected to the circular conversion in transmission geometry addressed above. Figure 8 depicts an example. Parameters correspond to those of Fig. 2. Notably, left-handed incident circular

#119965 - $15.00 USD Received 13 Nov 2009; revised 22 Dec 2009; accepted 28 Dec 2009; published 7 Jan 2010

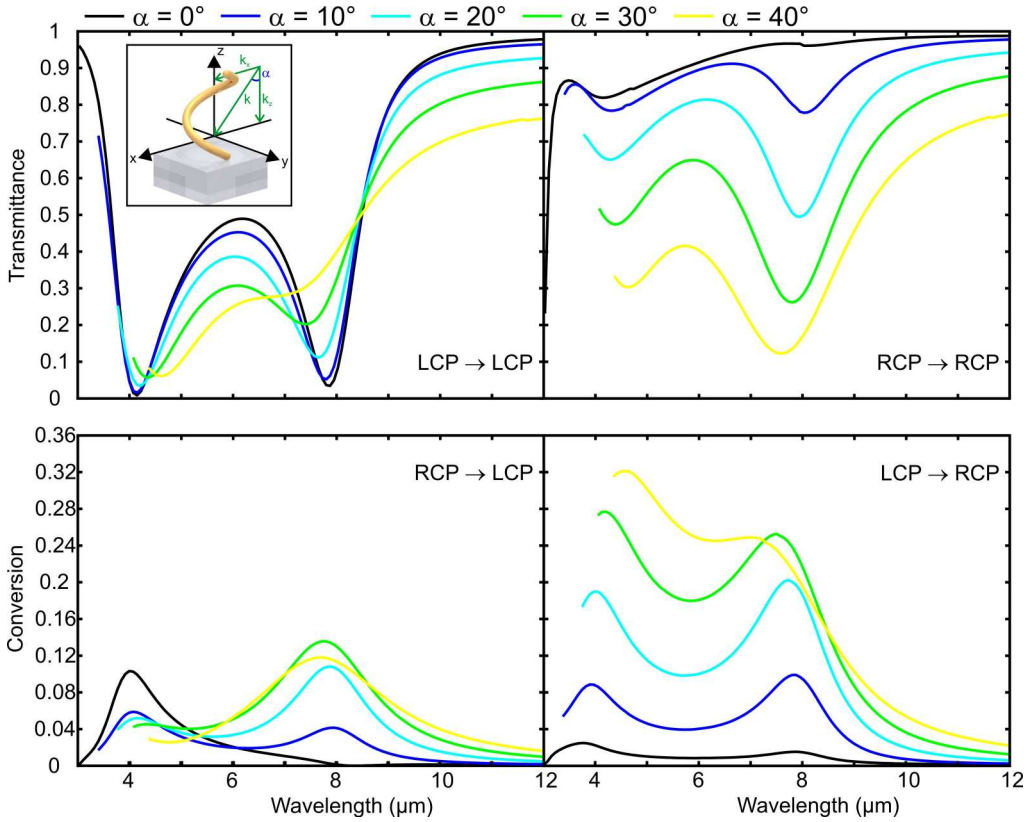

Fig. 7. As Fig. 2, $N = 1$, but the angle of incidence, α, is varied from normal incidence to 40 degrees with respect to the surface normal in steps of 10 degrees. The inset on the left-hand side illustrates the oblique-incidence geometry.

polarization is mainly reflected as left-handed circular polarization. This is just opposite to the behavior of a gold mirror (see dashed red curves in Fig. 8) or that of a usual dielectric half-space following Fresnel-type reflection [1]. There, the reflected light flips the handedness from left-handed to right-handed and vice versa upon 180 degrees change of the direction of the wave vector of light. The conversion behavior of the helices is also not expected for an ideal chiral medium [15,16]. Intuitively, we interpret this numerical finding as being due to the termination of the metal wire. The end of the wire together with the center of the helix defines an axis in real space that breaks the symmetry. Thus, in addition to pure circular dichroism, the structure also exhibits some degree of linear birefringence. This linear birefringence contributes to the observed circular polarization conversion in transmittance geometry. It also explains the non-Fresnel-type reflectance: If the relative phase between the two orthogonal linear components in the field reflection coefficients changes by 180 degrees, left-handed incident circular polarization turns into left-handed light. The stronger effects in reflectance than in transmittance are not really surprising as phase changes at a structure's surface usually have a much more profound effect on the reflection properties than on the transmission properties.

Notably, the spectra for LCP → RCP and RCP → LCP in Fig. 8 are very nearly identical – in sharp contrast to our above findings for transmittance. For normal incidence and for a medium exclusively exhibiting linear birefringence (and no circular dichroism at all), it is straightforward to show that the spectra for LCP → RCP and RCP → LCP are strictly

#119965 - $15.00 USD Received 13 Nov 2009; revised 22 Dec 2009; accepted 28 Dec 2009; published 7 Jan 2010

identical indeed. Thus, this finding again highlights the importance of linear birefringence for the reflectance spectra in Fig. 8. For oblique incidence (not shown), the spectra for LCP → RCP and RCP → LCP behave differently.

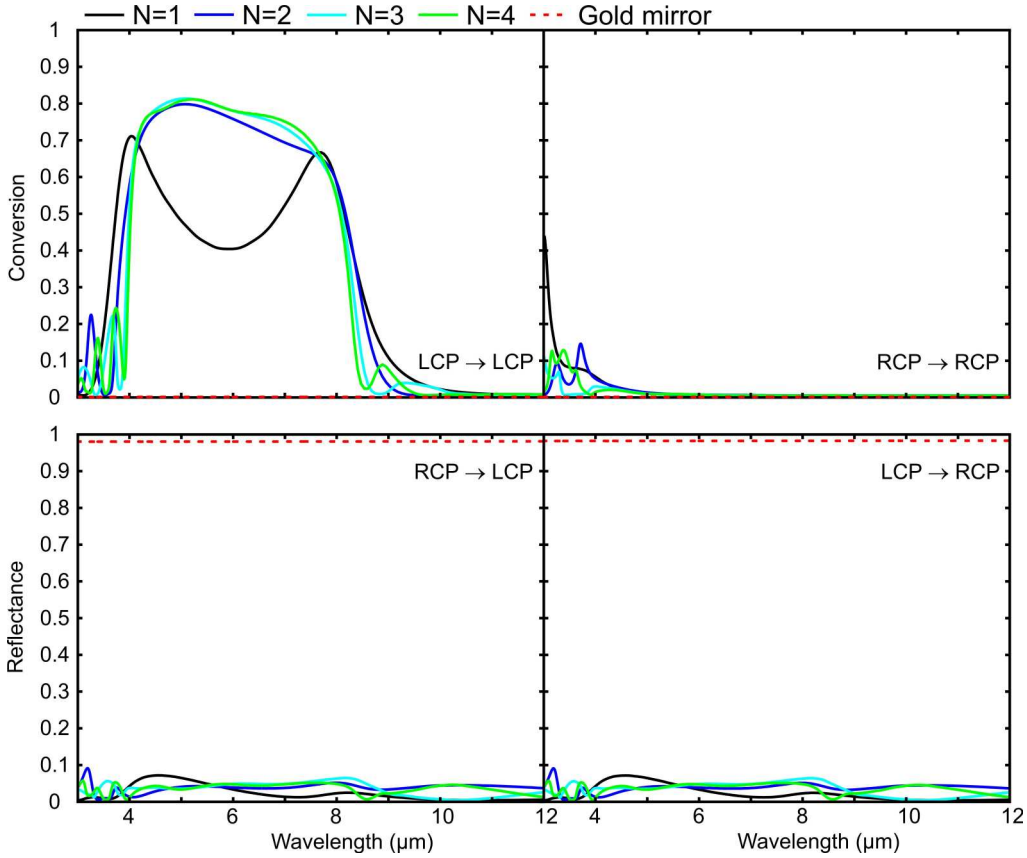

Fig. 8. Intensity reflectance and conversion spectra for the parameters and the geometry shown in Fig. 2. For usual Fresnel-type reflection, LCP (RCP) incident light turns into RCP (LCP) reflected light. Thus, in reflection geometry, by "conversion" we refer to, e.g., the ratio of LCP reflected light intensity and LCP incident light intensity. The red curves correspond to the behavior of an ideal metal mirror.

Finally, it is important to note that the discussed pronounced circular polarization conversion in reflection prohibits meaningful chiral effective-parameter retrieval along the lines of [16]. Hence, we have refrained from any retrieval in the present work.

3. Conclusion

In conclusion, we have systematically studied the optical properties of chiral metamaterials consisting of arrays of metal helices for propagation of light along the helix axis. The ideal structure for applications in terms of broadband circular polarizers is composed of metal helices with a diameter close but not too close to the square lattice constant, two or three helix pitches, a helix pitch comparable to or larger than the lattice constant, and a metal wire much thinner than the helix diameter (yet much thicker than the skin depth). The circular-polarizer behavior is fairly sensitive to deviations from normal incidence of light, i.e., to deviations from propagation along the helix axis.

#119965 - $15.00 USD Received 13 Nov 2009; revised 22 Dec 2009; accepted 28 Dec 2009; published 7 Jan 2010

Acknowledgments

We thank Michael Thiel and Costas M. Soukoulis for discussions. We acknowledge support by the Deutsche Forschungsgemeinschaft (DFG) and the State of Baden-Württemberg through the DFG-Center for Functional Nanostructures (CFN) within subproject A1.5. The project PHOME acknowledges the financial support of the Future and Emerging Technologies (FET) programme within the Seventh Framework Programme for Research of the European Commission, under FET-Open grant number 213390. The project METAMAT is supported by the Bundesministerium für Bildung und Forschung (BMBF). The research of S. L. is further supported through a Helmholtz-Hochschul-Nachwuchsgruppe (VH-NG-232). The PhD education of J.K.G. is embedded in the Karlsruhe School of Optics & Photonics (KSOP).

#119965 - $15.00 USD Received 13 Nov 2009; revised 22 Dec 2009; accepted 28 Dec 2009; published 7 Jan 2010